

Electronic Structure Information from Electron Impact Ionisation Experiments*

M. A. Coplan,^A J. P. Doering,^B D. H. Madison,^C J. H. Moore^A
and A. A. Pinkás^{B,D}

^A Institute for Physical Science and Technology and
Department of Chemistry and Biochemistry,
University of Maryland, College Park, MD 20742–2431, USA.

^B Department of Chemistry, Johns Hopkins University,
Baltimore, MD, USA.

^C Department of Physics, University of Missouri-Rolla,
Rolla, MO 65401, USA.

^D Present address: Department of Physics,
Jersey City State College, Jersey City, NJ, USA.

Abstract

Electron impact ionisation with full determination of the kinematics (measurement of energies and momenta of the incident, scattered and ejected electrons) has proven to be useful for investigating both the electronic structure of atoms and molecules and the mechanism of ionisation. These experiments are, by definition, coincidence experiments since it is necessary to be sure that all the detected electrons originate from the same collision. For single-electron ionisation, (e, 2e), the emphasis has been on momentum densities and spectroscopic factors—see for example Coplan *et al.* (1994), McCarthy and Weigold (1976, 1988, 1991) and Leung (1991). For double ionisation, (e, 3e), data are just beginning to emerge, with early results on the Auger process and direct double ionisation (Duguet and Lahmam-Bennani 1992). Both (e, 2e) and (e, 3e) experiments are technically challenging because the signals are small and there is usually a large background. In the last few years, electrostatic spectrographs and position sensitive detectors have improved the resolution and precision of (e, 2e) measurements and have made (e, 3e) measurements a practical reality.

1. Momentum Densities and Spectroscopic Factors

The theoretical basis of the determination of electronic structure from ionisation experiments is the plane wave Born approximation (McCarthy 1992) where the incident, scattered and ejected electrons are represented by plane waves and the incident electron interacts with only one target electron. The cross section for single ionisation within the plane wave Born approximation is given by

$$\frac{d^3\sigma}{d\Omega'_0 d\Omega_a dE} = \frac{m^2}{4\pi^2 \hbar^4} (k'_0 k_a / k_0) \left| \langle e^{ik_0 \cdot r} e^{ik'_a \cdot r_a} \psi'(r_b, \dots, r_n) \middle| \frac{-\epsilon^2}{|\mathbf{r} - \mathbf{r}_a|} | e^{ik_0 \cdot r} \psi(r_a, \dots, r_n) \rangle \right|^2, \quad (1)$$

* Refereed paper based on a contribution to the Advanced Workshop on Atomic and Molecular Physics, held at the Australian National University, Canberra, in February 1995.

where $e^{i\mathbf{k}_0 \cdot \mathbf{r}}$, $e^{i\mathbf{k}'_0 \cdot \mathbf{r}}$ and $e^{i\mathbf{k}_a \cdot \mathbf{r}_a}$ are plane waves representing the incident, scattered and ejected electrons with wave vectors \mathbf{k}_0 , \mathbf{k}'_0 and, \mathbf{k}_a and position coordinates \mathbf{r} and \mathbf{r}_a . Also, $\psi(\mathbf{r}_a, \mathbf{r}_b, \dots, \mathbf{r}_n)$ is the n -electron wave function for the target atom or molecule, and $\psi'(\mathbf{r}_b, \dots, \mathbf{r}_n)$ is the $(n-1)$ -electron wave function for the residual ion. The interaction that couples the initial to the final state is the Coulomb interaction, $-\epsilon^2/|\mathbf{r} - \mathbf{r}_a|$ between the incident electron and electron a of the target; ϵ is the electronic charge. After evaluating the integral (Inokouti 1971), the cross section reduces to

$$\frac{d^3\sigma}{d\Omega'_0 d\Omega_a dE} = \frac{4m^2\epsilon^4}{\hbar^4 K^4} (k'_0 k_a/k_0) |\langle \psi'(\mathbf{r}_b, \dots, \mathbf{r}_n) | e^{i\mathbf{q}_a \cdot \mathbf{r}_a} \psi(\mathbf{r}_a, \mathbf{r}_b, \dots, \mathbf{r}_n) \rangle|^2, \quad (2)$$

where \mathbf{K} is the momentum transfer wave vector and the wave vector of the residual ion is given by $\mathbf{q}_a = \mathbf{k}_0 - \mathbf{k}'_0 - \mathbf{k}_a$. If the net momentum of the target atom or molecule is zero before the collision, and the momentum transferred by the incident electron all goes to electron a , \mathbf{q}_a can be interpreted as the negative of the wave vector of electron a at the instant of the collision. If, furthermore, the target and residual ion wave functions can be written as single-electron product functions, $\phi_a(\mathbf{r}_a) \phi_b(\mathbf{r}_b) \phi_c(\mathbf{r}_c) \dots \phi_n(\mathbf{r}_n)$ and $\phi'_b(\mathbf{r}_b) \phi'_c(\mathbf{r}_c) \dots \phi'_n(\mathbf{r}_n)$, the cross section reduces to

$$\frac{d^3\sigma}{d\Omega'_0 d\Omega_a dE} = \frac{4m^2\epsilon^4}{\hbar^4 K^4} (k'_0 k_a/k_0) \times |\langle \phi_b(\mathbf{r}_b) \phi_c(\mathbf{r}_c) \dots \phi_n(\mathbf{r}_n) | \phi'_b(\mathbf{r}_b) \phi'_c(\mathbf{r}_c) \dots \phi'_n(\mathbf{r}_n) \rangle|^2 |e^{i\mathbf{q}_a \cdot \mathbf{r}_a} \phi_a(\mathbf{r}_a)|^2. \quad (3)$$

The first integral is the overlap between the wave function for the initial state with a hole in the ϕ_a orbital and the final ion state. The square of this integral is the spectroscopic factor. The second integral is the Fourier transform of the single electron orbital ϕ_a . The square of this integral is the orbital momentum density, $\rho(\mathbf{q})$. From (e,2e) measurements it is therefore possible to obtain spectroscopic factors and single electron orbital momentum densities if conditions can be arranged so that the plane wave Born approximation applies. In general this means incident electron energies sufficiently large so that both the scattered and ejected electrons have kinetic energies between 10 and 100 times the binding energy of the ejected electron, and the selection of only those collisions where all of the energy lost by the incident electron is transferred to the ejected electron. There are several experimental arrangements that satisfy these conditions (see for example Coplan 1994), but the most frequently used is the noncoplanar symmetric where the energies of the scattered and ejected electrons are arranged to be half the difference between the incident energy and binding energy of the ejected electron.

Our research has mainly been concerned with momentum densities and the relation between them and the physical and chemical properties of atoms and molecules. We have been led to this because momentum densities are only a phase factor and Fourier transform away from the wave function from which all observable properties of atoms and molecules can, in principle, be obtained.

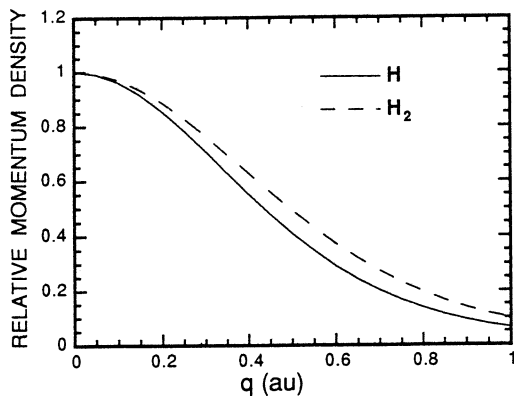


Fig. 1. Momentum densities for the 1s electron of the hydrogen atom and the $\sigma 1s$ electron of the hydrogen molecule.

In this regard, it is useful to examine momentum densities for different but related species. Fig. 1 shows the momentum densities for the 1s electron of the hydrogen atom and the $\sigma 1s$ electron of the hydrogen molecule. The two species are very different, with different energy level structures and chemical and physical properties, yet their momentum densities differ by at most a few per cent. Another example is the highest occupied molecular orbital of benzene and the fluorobenzenes (Subramaniam 1994). Fig. 2 shows the experimentally determined spherically averaged momentum densities for benzene, monofluorobenzene, difluorobenzene, trifluorobenzene, and hexafluorobenzene. In spite of the different chemical composition, symmetry, chemical and physical properties, the momentum densities are very much alike. There are, of course, many other examples where the differences are larger, but in general, it is necessary to perform (e, 2e) experiments with accuracies of a few per cent to get meaningful information about wave functions. There are obstacles to obtaining such accuracy, some are instrumental while others have their origin in the very nature of the targets and electron scattering. Instrumental limitations come from the relatively low target densities that can be produced in the gas phase, background electrons scattered from the surfaces of the spectrometer, mechanical misalignment of the scattered and ejected electron detectors so that both are not viewing identical collision volumes, magnetic fields that must be maintained at milligauss levels, fluctuations in the outputs of the electron and target gas sources, and drifts in the gains of the electron detectors. These difficulties are compounded by the fact that electron impact ionisation cross sections are small, especially at the energies where the plane wave Born approximation can be used. In addition, in order to discriminate among the different electrons in a target, it is necessary to have sufficient energy resolution. For atomic targets, resolutions of a few eV are sufficient, but for molecules where electronic states are closer together, resolutions of 0.5 eV or better are desirable, but difficult to attain.

An important experimental limitation for gas phase molecular targets lies in the fact that all orientations of the target with respect to the incident electron are equally probable. For this reason the experimental momentum densities are spherical averages, as shown in Fig. 2. For molecules, where spherical symmetry

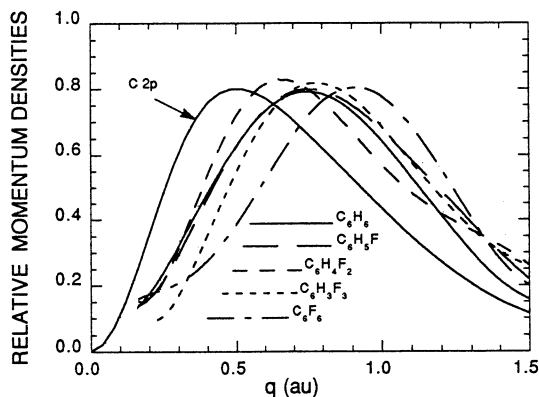


Fig. 2. Comparison of spherically averaged experimental momentum densities for benzene, monofluorobenzene, difluorobenzene, trifluorobenzene and hexafluorobenzene. For reference, the calculated momentum density of the 2p electron of carbon is shown.

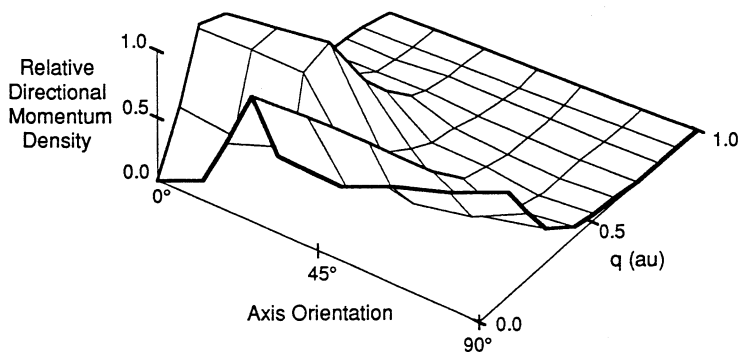


Fig. 3. Oriented momentum densities for the π_u outermost orbital of N_2 . The densities are shown as a function of angle with respect to the molecular axis.

is rare, information is lost by averaging. As an example, Fig. 3 shows the momentum densities for the π_u outermost orbital of the nitrogen molecule as a function of orientation with respect to the molecular axis. There is a great deal more information available from these directional momentum densities than the spherically averaged density, which has a node at the origin of momentum space and a maximum near 0.6 momentum units. We have recently examined a scheme for obtaining directional momentum densities for linear molecules. A schematic drawing of the method is shown in Fig. 4. The method applies to those ionising collisions that leave the residual ion in a dissociating state, and relies on detection of the products of the dissociation of the residual ion in coincidence with the scattered and ejected electrons. Because dissociation is along a bond, the detection of the dissociation products is sufficient to establish

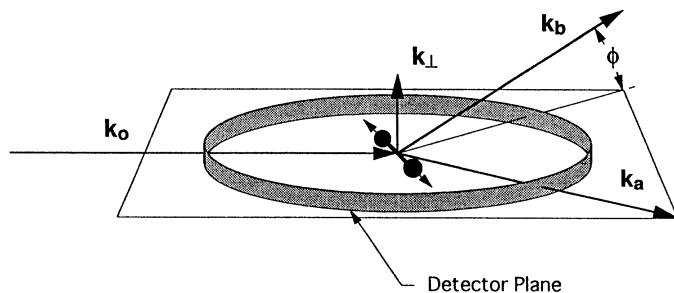


Fig. 4. Proposed method for determining directional momentum densities. Detectors in the scattering plane collect the products of the dissociation of the residual ion after an $(e, 2e)$ event. The detection of the ion products in triple coincidence with the scattered and ejected electrons gives the orientation of the molecular axis at the instant of ionisation as well as the momentum of the ejected electron.

the orientation of the residual molecular ion at the instant of dissociation. The fact that dissociation occurs on a time scale that is short compared to rotation means that knowledge of the orientation of the ion is sufficient to establish the orientation of the target at the instant of ionisation. The implementation of this technique requires modification of the ordinary $(e, 2e)$ spectrometer and the addition of triple coincidence detection circuits. Because the signals are expected to be small, it is necessary to use multiple detectors to increase the data rates to acceptable levels.

While spherical averaging results in a loss of information, over-simplification of the scattering process itself can lead to incorrect interpretations of experimental cross sections. The literature is replete with experimental data and calculations for many different targets over a wide range of energies showing variations of cross sections from those predicted by the plane wave theory. What has been missing, however, is a consistent set of measurements of $(e, 2e)$ cross sections for a series of targets over a wide energy range using the noncoplanar geometry and a single instrument. We have undertaken such measurements with the goal of determining the size and nature of the deviations from the plane wave theory. We have chosen simple targets where the wave functions and momentum densities are well known. The noncoplanar symmetric geometry has been the geometry of choice for electronic structure determinations because of the ease with which relative experimental cross sections can be converted to momentum densities. For other geometries, the experimental cross sections must be corrected for the change in the electron-electron cross section with scattering angle before momentum densities can be extracted from the data (McCarthy and Weigold 1976).

The systems investigated are He, Ne, Ar and H_2 over an incident electron energy range from approximately 100 to 1000 eV (Pinkás 1994). In Fig. 5 are the results for the 2p orbital of neon at (a) 121 and (b) 921 eV incident electron energy. In the figure, experimental cross sections are compared with the 2p momentum density (plane wave theory) and distorted wave Born approximation calculations (Madison *et al.* 1989). Fig. 6 shows experimental cross sections for the 3p electron of argon and the calculated momentum density (plane wave

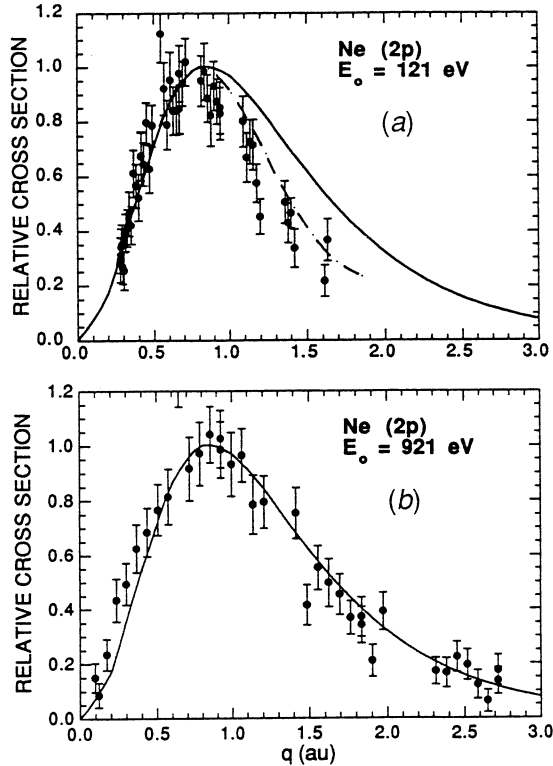


Fig. 5. Experimental and calculated (e, 2e) cross sections in the symmetric noncoplanar geometry for the 2p electron of neon at incident electron energies of (a) 121 eV and (b) 921 eV. The calculated momentum density of the 2p electron (plane wave theory) is shown as a solid curve for both incident energies. The calculated cross section based on the distorted wave Born approximation is shown as a broken curve for the 121 eV case. For the 921 eV case, the DWBA calculations are indistinguishable from the plane wave results.

theory) and DWBA results. We see that the deviations from the plane wave theory are substantial at low energy—well in excess of 5%. We also see that the deviations as a function of incident energy are very different for the two targets. At approximately 100 eV the deviations from the plane wave theory at about one momentum unit are in the range of 30% for neon and close to 100% for argon. At approximately 900 eV the neon data agree with the plane wave theory except at the highest momentum values, while for argon the deviations are of the order of several per cent at momentum values as small as 1 momentum unit. DWBA calculations agree with the experimental data for neon over the full incident electron range, and similar calculations for argon are also within experimental uncertainty for q values less than 1 momentum unit. Above 1 momentum unit the distorted wave results increase while the measured cross section decreases. This increase in the DWBA cross section is thought to be an artifact of the calculation. This can be understood in terms of the interactions that exist during electron impact ionisation. These are shown in Fig. 7. The plane wave

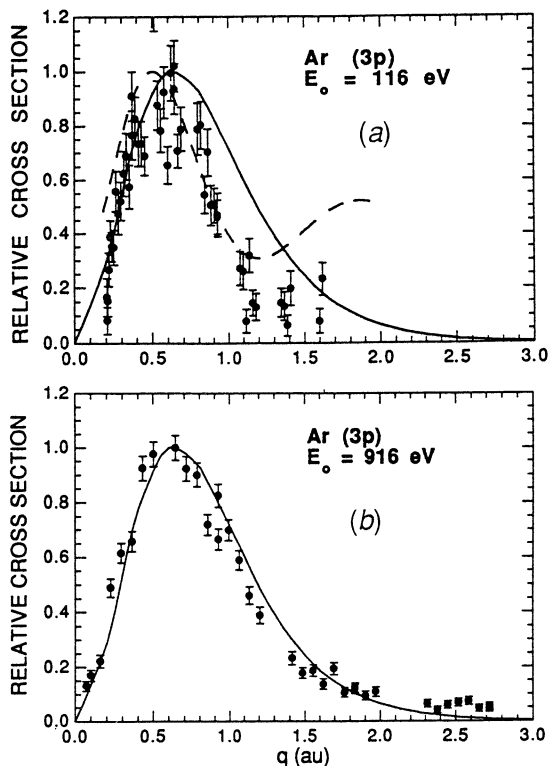


Fig. 6. Experimental and calculated ($e, 2e$) cross sections in the symmetric noncoplanar geometry for the 3p electron of argon at incident electron energies of (a) 116 eV and (b) 916 eV. The calculated momentum density of the 3p electron (plane wave theory) is shown as a solid curve for both incident energies. The calculated cross section based on the DWBA is shown as a broken curve for the 116 eV case. The large increase in the distorted wave results at q values above 1.0 a.u. is thought to be an artifact of the calculation. For the 916 eV case, the DWBA calculations are indistinguishable from the plane wave results.

Born approximation neglects all interactions except v_1 , the Coulomb interaction of the incident electron with the target electron. The DWBA accounts for the interactions between the incident electron and the target and the ejected electron and scattered electrons and the residual ion through the use of distorted, rather than plane waves for the unbound electrons. In general, at incident electron energies above 1000 eV, ($e, 2e$) cross sections can be reliably interpreted in terms of momentum densities, but for lower energies the deviations become substantial. Moreover, the magnitude of the deviations are very much dependent on the nature of the target, and there is no simple way to predict, at energies below 1000 eV, the degree to which momentum densities can be extracted from ($e, 2e$) cross sections without a distorted wave calculation. This is an even more serious situation for molecular targets where distorted wave calculations have yet to be performed.

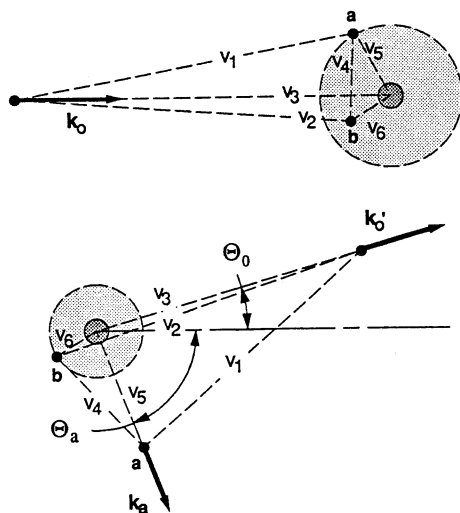


Fig. 7. Schematic diagrams of the interactions during electron impact ionisation. The top drawing shows the initial state, and the bottom drawing shows the final state. The interactions are labeled v_1 through v_6 and represent the interaction between the incident electron and target electron a (v_1), the incident electron and atomic electron b (v_2), the incident electron and the atomic nucleus (v_3), the interaction between electrons a and b (v_4), and the interactions between electrons a and b with the nucleus (v_5 and v_6). The angle Θ_0 is the angle through which the incident electron is scattered, and Θ_a is the angle of ejection of the target electron. The angles are measured with respect to the direction of the incident electron. The plane wave Born approximation neglects all interactions except v_1 , the Coulomb interaction of the incident electron with the target electron. The distorted wave Born approximation accounts for the interactions between the incident electron and the target, and the ejected electron and scattered electrons and the residual ion, through the use of distorted, rather than plane waves for the unbound electrons.

2. Double Ionisation and Electron Correlation

While single electron impact ionisation provides information about single electron momentum densities, under the appropriate experimental conditions, double ionisation can give information about the distribution of relative momenta of the two ejected electrons at the instant of ejection. Double ionisation involving the ejection of two electrons by a single incident electron was first suggested nearly thirty years ago by Glassgold and Ialongo (1968) who, in their paper on the $(e, 2e)$ reaction, noted that the correlated motion of atomic electrons could possibly be observed with an $(e, 3e)$ experiment. In such an experiment, which is fully differential in the angles and energies of the incident scattered and ejected electrons, the scattered and two ejected electrons are detected in triple coincidence, while their energies and momenta are also determined. The geometry and kinematics of an $(e, 3e)$ event are shown in Fig. 8. The incident electron has energy E_0 and wave vector k_0 . The scattered electron, emerging from the collision at an angle of Θ_0 to the incident electron direction, has energy E_0' and wave vector k_0' . The two ejected electrons leave the collision at angles

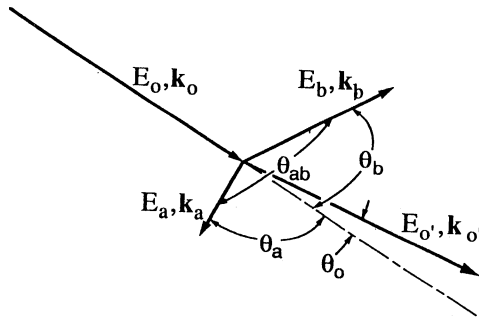


Fig. 8. The (e, 3e) geometry: the incident electron has energy E_0 and wave vector \mathbf{k}_0 . The scattered electron has energy E'_0 and wave vector \mathbf{k}'_0 . The ejected electrons have energies E_a and E_b . The incident electron is scattered through angle θ_0 and the ejected electrons leave the collision at angles θ_a and θ_b with respect to the direction of the incident electron. The angle between the ejected electrons is θ_{ab} .

θ_a and θ_b with respect to the incident electron direction and have energies E_a and E_b and wave vectors \mathbf{k}_a and \mathbf{k}_b respectively. The angle between the two ejected electrons is θ_{ab} . By analogy with the single ionisation case, if the incident, scattered and ejected electrons can all be represented by plane waves, the cross section for double ionisation has the form

$$\frac{d^5\sigma}{d\Omega'_0 d\Omega_a d\Omega_b dE_a dE_b} = \frac{m^2}{4\pi^2\hbar^4} (k'_0 k_a k_b/k_0) \times \left| \left\langle e^{i\mathbf{k}'_0 \cdot \mathbf{r}} e^{i\mathbf{k}_a \cdot \mathbf{r}_a} e^{i\mathbf{k}_b \cdot \mathbf{r}_b} \psi'(\mathbf{r}_c, \dots, \mathbf{r}_n) \middle| \frac{-\epsilon^2}{|\mathbf{r} - \mathbf{r}_a|} \middle| e^{i\mathbf{k}_0 \cdot \mathbf{r}} \psi(\mathbf{r}_a, \mathbf{r}_b, \dots, \mathbf{r}_n) \right\rangle \right|^2. \quad (4)$$

This is the simple ‘single hit’ model for double ionisation. Performing the integration over the coordinates of the incident electron, and noting that $\mathbf{q}_a + \mathbf{q}_b = -\mathbf{k}_0 + \mathbf{k}'_0 + \mathbf{k}_a + \mathbf{k}_b$, we have

$$\frac{d^5\sigma}{d\Omega'_0 d\Omega_a d\Omega_b dE_a dE_b} = \frac{m^2}{4\pi^2\hbar^4} (k'_0 k_a k_b/k_0) \times \left| \langle \psi'(\mathbf{r}_c, \mathbf{r}_d, \dots, \mathbf{r}_n) | e^{i(\mathbf{q}_a + \mathbf{q}_b) \cdot \mathbf{r}_a} e^{i\mathbf{k}_b \cdot (\mathbf{r}_a - \mathbf{r}_b)} \psi(\mathbf{r}_a, \mathbf{r}_b, \dots, \mathbf{r}_n) \rangle \right|^2. \quad (5)$$

For uncorrelated single-electron product wave functions the cross section vanishes; however, if the target function can be written as the product of two-electron wave functions $\xi_{ij}(\mathbf{r}_i, \mathbf{r}_j)$ we have the result

$$\frac{d^5\sigma}{d\Omega'_0 d\Omega_a d\Omega_b dE_a dE_b} = \frac{m^2}{4\pi^2\hbar^4} (k'_0 k_a k_b/k_0)$$

$$\begin{aligned} & \times |\langle X'_{c,\dots,n}(\mathbf{r}_c, \dots, \mathbf{r}_n) | \xi_{c,d}(\mathbf{r}_c, \mathbf{r}_d), \dots, \xi_{n-1,n}(\mathbf{r}_{n-1}, \mathbf{r}_n) \rangle|^2 \\ & \times |\langle e^{i(\mathbf{q}_a + \mathbf{q}_b) \cdot \mathbf{r}_a} e^{i\mathbf{k}_b \cdot (\mathbf{r}_a - \mathbf{r}_b)} \xi_{a,b}(\mathbf{r}_a, \mathbf{r}_b) \rangle|^2, \end{aligned} \quad (6)$$

where $X'_{c,\dots,n}(\mathbf{r}_c, \dots, \mathbf{r}_n)$ is the $n-2$ electron ion wave function. In this simple formulation, the probability of observing a non-zero cross section depends on the degree of correlation in the two-electron wave function. Instead of a simple Fourier transformation of the ejected electron wave function, we have a double Fourier transform of the two-electron wave function. The transform depends on the sum of the momenta of the ejected electrons and the difference of their position coordinates. The physical interpretation of this transform is more difficult than for the case of single ionisation, but it is nevertheless possible to calculate (e, 3e) cross sections for a range of correlated wave functions. An interesting case is the direct double ionisation of magnesium by electron impact. Magnesium is a quasi-two electron atom (two 3s electrons outside of a closed shell), and there is a large amount of spectroscopic and photoionisation data that show significant correlation for the outer valence electrons. The calculated cross section for double ionisation at an incident electron energy of 3652 eV is shown in Fig. 9. The calculation (Ceraulo *et al.* 1994) uses the highly correlated CI wave function of Krause and Berry (1985) for the ground state of the atom, with a pseudopotential for the electronic core (Bachelet *et al.* 1982). The final state interactions between the ejected electrons are accounted for through the introduction of a term that vanishes when the distance between the ejected electrons is zero. This is called the Coulomb hole. It is important to note that even for this case of highly correlated electrons the cross section is small and requires a spectrometer very much different from conventional (e, 2e) units.

The spectrometer we have constructed for double ionisation measurements in magnesium is shown in Fig. 10. It consists of an electron source, an oven for the production of a beam of magnesium atoms, a scattered-electron analyser, and two ejected-electron analysers (Ford *et al.* 1995*a, b*). Because of the small cross section for direct double ionisation, we use a configuration with up to eight ejected-electron detectors spaced around the focal planes of the two ejected-electron analysers. In this way we can observe 64 different combinations of angles for the ejected electrons at a fixed angle for the scattered electron.

The first measurements with the spectrometer were not of direct double ionisation, in magnesium, but rather of a more probable Auger process. The Auger process we chose was the ejection of a 2p electron with the subsequent filling of the hole with a 3s electron and the simultaneous ejection of a second, 35 eV 3s Auger electron to produce a doubly-charged magnesium ion in its ground state (Schmidt 1990). The incident electron energy was 3500 eV, and the scattered electron was detected at 0° scattering angle. The angular distributions of the ejected and Auger electrons were measured for ejected electron energies of 35, 45 and 100 eV. The results are shown in Fig. 11 for the case where the ejected and Auger electrons have identical energies. The angle Θ_{ab} is the included angle between the two electrons independent of the direction of ejection of either ejected electron. The data show a clear minimum in the relative cross

$E_0 = 3652 \text{ eV}$, $\Theta_0 = 1^\circ$
 $E_a = 65 \text{ eV}$, $E_b = 65 \text{ eV}$
 Coulomb Hole Final State

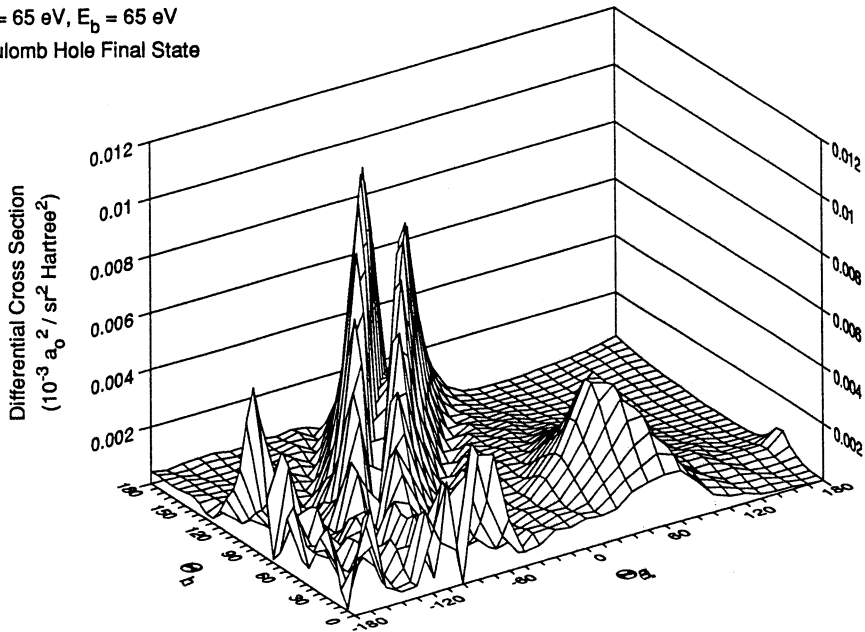


Fig. 9. Calculated $(e, 3e)$ cross sections in atomic units for the direct double ionisation of magnesium at an incident electron energy of 3652 eV. In this calculation the angle of scatter of the incident electron is held at 1° . The angle of ejection of electron a , Θ_a , is measured with respect to the incident electron direction and can vary from -180° to 180° . The angle of ejection of electron b , Θ_b , is also with respect to the incident beam direction and can vary from 0° to 180° . The largest values of the cross section occur for Θ_{ab} approximately equal to 180° .

section at 90° . The results can be explained in terms of the alignment of the initially created singly charged ion by the incident and ejected electrons. This alignment is related to the transfer of angular momentum to the ion in the initial ionisation and affects the angular distribution of the Auger electron relative to the ejected electron. The solid curve in the figure is the best fit to the function

$$1 + \beta_a P_2(\cos\Theta_a) + \beta_b P_2(\cos\Theta_b) + \beta_{ab} P_2(\cos\Theta_{ab}), \quad (7)$$

where β_a , β_b and β_{ab} are the adjustable parameters. This function is based on a model of Schmidt (1990) for the joint angular distribution of Auger and photoelectrons. The derived values of β_a , β_b and β_{ab} are in agreement with those from theoretical calculations using the formulas of Kabachnik (1992).

After completing the Auger work, we began direct ionisation experiments. It is important to note that the cross section is a strong function of the incident electron energy, falling at least as fast as $1/E_0^2$. The cross section is also a strongly decreasing function of the energies of the ejected electrons. We have first performed an $(e, (3-1)e)$ experiment, that is, an $(e, 3e)$ experiment where the third electron is not collected. We have done the experiment with an incident-electron energy of 1000 eV and ejected-electron energies of (20 eV, 20 eV) and (20 eV,

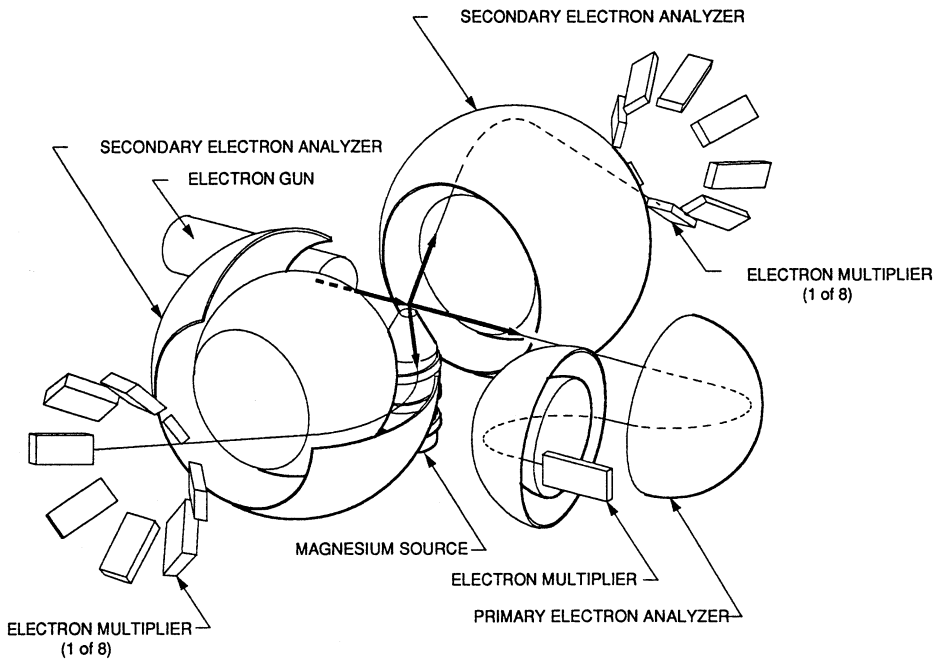


Fig. 10. Perspective view of the multiple detector (e, 3e) spectrometer showing analysers, detectors, electron source and magnesium oven.

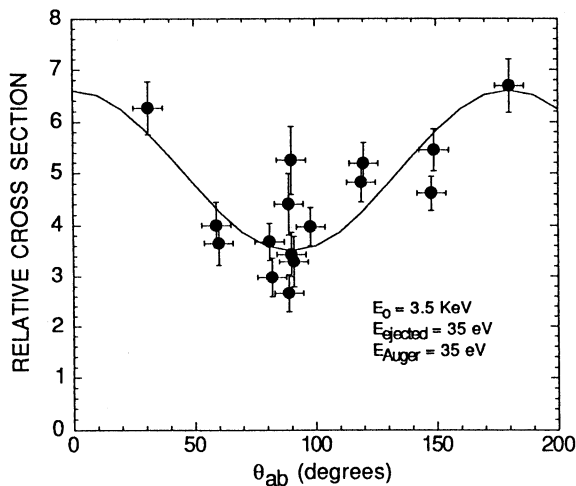


Fig. 11. Angular distributions for the ejected and Auger electrons in magnesium.

80 eV). Preliminary results indicate a cross section that is approximately two to three orders of magnitude smaller than the Auger cross sections at comparable incident electron energies. The observation of the (e, (3-1)e) signal gives us some confidence that we will be able to perform the full (e, 3e) experiment and extract information about electron correlation in magnesium.

3. Summary and Conclusions

The (e, 2e) experiments, while providing information about electron momentum densities in atoms and molecules, are nevertheless sensitive to interactions other than that of the incident electron with the target electron. The effect of the interactions is to partially destroy the correspondence between cross sections and momentum densities. Distorted wave calculations are successful in accounting for the variation in the cross sections for atomic targets over a wide energy range, but for molecular targets the calculations are at the limit of current capabilities. For molecules there is the additional loss of information from spherical averaging. This can be overcome in certain cases for linear molecules.

Double ionisation experiments are very sensitive to electron correlation, but the cross sections are small and the interactions of the electrons and the ion core can distort the angular distribution. In spite of these difficulties, (e, 3e) experiments are now producing data on the Auger process and the direct double ionisation of atoms.

Acknowledgments

This work was supported by NSF Grants PHY-91-07337, PHY 91-16199 and CHE-88-08589. Additional support was provided by NATO collaborative Research Grant No. CRG 920101 and by the University of Maryland through a University of Maryland Faculty Research Award (JHM).

References

- Bachelet, G. B., Hamann, D. R., and Schlüter, M. (1982). *Phys. Rev. B* **26**, 4199.
Ceraulo, S. C., Stehman, R. M., and Berry, R. S. (1994). *Phys. Rev. A* **49**, 1730.
Coplan, M. A., Moore, J. H., and Doering, J. P. (1994). *Rev. Mod. Phys.* **66**, 985.
Duguet, A., and Lahmam-Bennani, A. (1992). *Z. Phys. D* **23**, 383–8.
Ford, M. J., Coplan, M. A., Moore, J. H., and Doering, J. P. (1995a). *Rev. Sci. Instrum.* **66**, 3137.
Ford, M. J., Doering, J. P., Coplan, M. A., Cooper, J. W., and Moore, J. H. (1995b). *Phys. Rev. A* **51**, 418.
Glassgold, A. E., and Ialongo, G. (1968). *Phys. Rev.* **178**, 151.
Inokouti, M. (1971). *Rev. Mod. Phys.* **43**, 297.
Kabachnik, N. M. (1992). *J. Phys.* **B25**, L369.
Krause, J. L., and Berry, R. S. (1985). *J. Chem. Phys.* **83**, 5153.
Leung, K. T. (1991). In 'Theoretical Models of Chemical Bonding', Part 3, Molecular Spectroscopy, Electronic Structure, and Intramolecular Interactions (Ed. Z. Maksic), p. 339 (Springer: Berlin).
McCarthy, I. E. (1992). *Z. Phys. D* **23**, 287–93.
McCarthy, I. E., and Weigold, E. (1976). *Phys. Rep. C* **27**, 275.
McCarthy, I. E., and Weigold, E. (1988). *Rep. Prog. Phys.* **51**, 299.
McCarthy, I. E., and Weigold, E. (1991). *Adv. Atom. Mol. Opt. Phys.* **27**, 201.
Madison, D. H., McCarthy, I. E., and Zhang, X. (1989). *J. Phys. B* **22**, 2041.
Pinkás, A. A. (1994). Ph.D. Thesis, University of Maryland.
Schmidt, V. (1990). In 'X-ray and Inner-shell Processes', AIP Conf. Proc. No. 215 (Eds T. A. Carlson *et al.*), pp. 559–81 (AIP: New York).
Subramaniam, C. K. (1994). Ph.D. Thesis, University of Maryland.

